Journal of Electroceramics 3:3, 255–260, 1999

Chemical Solution Deposition of Epitaxial $La_{1-x}(Ca, Sr)_xMnO_3$ Thin Films

ULRICH HASENKOX, CARSTEN MITZE & RAINER WASER
Institut für Werkstoffe der Elektrotechnik II, Aachen University of Technology, Templergraben 55, 52056 Aachen, Germany

R. ROBBERT ARONS
Institut für Elektrokeramische Materialien, Forschungszentrum Jülich, 52425 Jülich, Germany

JENS POMMER & GERNOT GÜNTHERODT
2. Physikalisches Institut, Aachen University of Technology, Templergraben 55, 52056 Aachen, Germany

Submitted July 30, 1998; Accepted October 8, 1998

Abstract. We report on the epitaxial growth of magnetoresistive $La_{0.7}Ca_{0.3}MnO_3$ and $La_{0.7}Sr_{0.3}MnO_3$ thin films by chemical solution deposition. Thin films were prepared by spin-coating of single-crystal $LaAlO_3$ (100) substrates with precursor solutions of different concentrations and crystallized at 850°C. The structure of the thin film was found to be influenced by the concentration of the spin-coating solution. The thin film structure and epitaxy was clearly improved by reducing the concentration of the precursor solution. All thin films displayed excellent electrical properties such as a low resistivity and very high metal-insulator transition temperatures T_{MI}.

Keywords: chemical solution deposition, epitaxial thin films, $La_{1-x}(Ca, Sr)_xMnO_3$, magnetoresistance

Introduction

The growth of epitaxial ceramic thin films prepared by Chemical Solution Deposition (CSD) has been extensively studied over the last years. Subjects of research were the relationship between substrate and thin film, the initiation of crystallization, the growth mechanisms of the epitaxial thin films, and the growth conditions [1–3]. One of the most important factors is the relationship between used substrate material and the crystal structure of the deposited thin film. If the lattice mismatch between both structures is small enough, epitaxy can occur. Usually, the substrate is chosen in order to minimize the lattice mismatch, although epitaxial thin films have been grown by CSD on substrates with a lattice mismatch as much as 16% [2]. Crystallization of the epitaxial thin film starts at the substrate-film interface with the formation of nanosized epitaxial grains. From these initial grains, the film grows to the surface at higher temperatures. The driving force for such a crystallization mechanism is the reduction of free energy by avoiding or eliminating grain boundaries [1,3].

Epitaxial thin films of $La_{1-x}Ca_xMnO_3$ or $La_{1-x}Sr_xMnO_3$ have been prepared over the last few years by a number of methods such as Pulsed Laser Deposition [4–6], sputtering [7–9] or MOCVD [10,11] and CSD [12,13]. Much of this recent research has been inspired by the discovery of the Colossal Magnetoresistance Effect (CMR) by von Helmolt et al. [14] and Jin et al. [15] which offers future possible applications as novel magnetic read heads [16] or positioning sensors [17]. Commonly used substrates are single-crystal $LaAlO_3$ (lattice constant 3.79 Å) or $SrTiO_3$ (lattice constant 3.90 Å) since their lattice constants are very close to values reported for $La_{0.7}Ca_{0.3}MnO_3$ (3.86 Å) [18] and $La_{0.7}Sr_{0.3}MnO_3$ (3.89 Å) [19]. Such thin films are frequently annealed

Correspondence should be addressed to: Prof. Rainer Waser, RWTH Aachen, Institut für Werkstoffe der Elektrotechnik II, Sommerfeldstr. 24, 52074 Aachen, Tel.: 0049 241 80 7812, Fax: 0049 241 8888 300, E-mail: waser@iwe.rwth-aachen.de

at temperatures around 850–950°C for several hours in air or oxygen to achieve complete crystallization and to adjust the oxygen stoichiometry [11,20,21]. Characteristic values with respect to the electrical properties are the transition temperature where the conduction behavior changes from a metallic to a semiconducting behavior, called T_{MI} for metal-insulator transition, and the magnetic Curie temperature T_C where the ferromagnetic coupling within the material ceases to exist. Typical values of T_{MI} reported for epitaxial $La_{0.7}Ca_{0.3}MnO_3$ thin films deposited on $LaAlO_3$ are 260 K [11] to 280 K [7]. For $La_{0.7}Sr_{0.3}MnO_3$, values of 375 K [4] up to 455 K [11] are observed.

Experimental

Thin films of $La_{0.7}Ca_{0.3}MnO_3$ (LCM) and $La_{0.7}Sr_{0.3}MnO_3$ (LSM) were deposited on polished single-crystal $LaAlO_3$ (100) substrates (Crystec GmbH, Berlin) by CSD. Size of the substrates was 10 mm × 10 mm. The coating solutions were prepared by dissolving stoichiometric amounts of the metal propionates of La, Sr, Ca and Mn in propionic acid with a final concentration of 0.3 M with respect to the Mn compound. The metal propionates were prepared by an exchange reaction starting from metal acetates, propionic acid and propionic anhydride. A more detailed description of the experimental procedure is given in reference [22]. Thin films were deposited from two different solutions with concentrations of 0.3 and 0.1 M, respectively. The less concentrated solution was prepared by diluting the 0.3 M precursor solution with a 1:1 mixture of propionic acid: 1-butanol. The addition of 1-butanol improved the spin coating properties of the diluted solution. Thin films were deposited at 4000 rpm for 30 s on a commmercially available resist spinner. Wet films were introduced into a preheated furnace after each coating and crystallized at 850°C for 30 min in oxygen atmosphere. Six coating-firing cycles were carried out. Analysis of the crystal structure was performed by means of a Philips PW3020 diffractometer. Electrical properties were measured with the standard four-point technique. Electrical contacts were formed with silver paint.

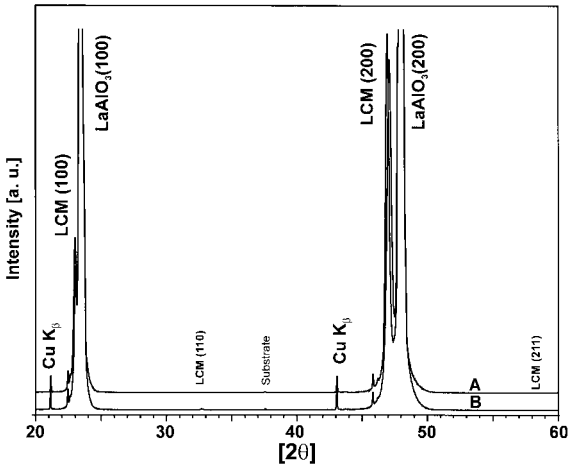

Fig. 1. XRD pattern (θ–2θ scan) of $La_{0.7}Ca_{0.3}MnO_3$ thin films deposited at 850°C on $LaAlO_3$ (100) substrates. Curve A: Film deposited from a 0.1 M precursor solution, Curve B: Film deposited from a 0.3 M precursor solution.

Results and Discussion

Structural properties

Figure 1 shows the XRD patterns of θ–2θ scans of $La_{0.7}Ca_{0.3}MnO_3$ thin films deposited on $LaAlO_3$. Curve A displays the pattern of a film obtained from a 0.1 M precursor solution, whereas curve B belongs to the film from a 0.3 M precursor solution. In curve A, only the reflections of the $LaAlO_3$ substrate and additional peaks of the ceramic layer (LCM) can be seen. The peak positions at 2θ-values of 23.013, 46.946 and 73.382° correspond to the (100), (200), and (300) reflections, leading to a lattice constant of 3.862 Å. Such a value is in very good agreement with a lattice constant of 3.86 Å reported in the literature [18]. The thin film in curve B, which was prepared from a solution of higher concentration (0.3 M), shows some additional, very small peaks in the diffraction pattern at 2θ-values of 32.725, 40.402, 58.541 and 68.730°, that can be indexed to the (110), (111), (211) and (220) reflections of $La_{0.7}Ca_{0.3}MnO_3$. Furthermore, the 2θ-values of the (100), (200) and (300) peaks are slightly shifted to 23.065, 47.106 and 73.765°, corresponding to a lattice constant of 3.854 Å. The small difference in the lattice constants could be caused by the different film thicknesses, the 110 nm film being more compressed in the *a*-*b*-plane leading to an elongation of the *c*-axis, whereas the film from the 0.3 M precursor solution could have more

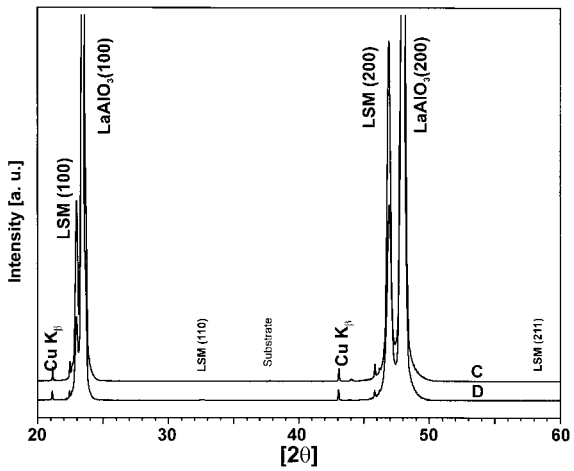

Fig. 2. XRD pattern (θ–2θ scan) of $La_{0.7}Sr_{0.3}MnO_3$ thin films deposited at 850°C on $LaAlO_3$ (100) substrates. Curve C: Film deposited from a 0.1 M precursor solution, Curve D: Film deposited from a 0.3 M precursor solution.

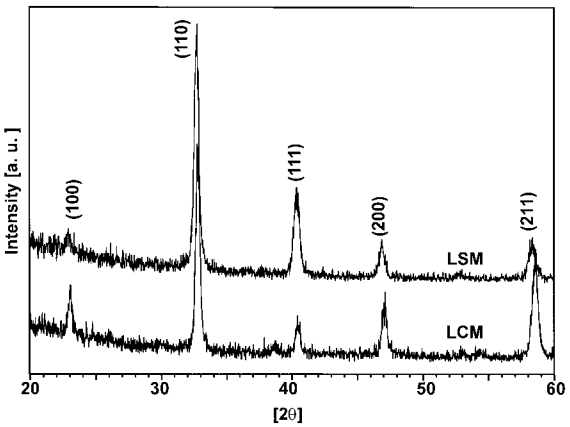

Fig. 3. Glancing incidence XRD pattern (incidence angle 1°) of a $La_{0.7}Ca_{0.3}MnO_3$ and a $La_{0.7}Sr_{0.3}MnO_3$ thin film deposited at 850°C from a 0.3 M precursor solution. The reflections of a small fraction of polycrystalline material can be seen. The intensity of the reflections is close to the noise level.

space to release stress due to the higher film thickness. Similar XRD patterns are observed for thin films with a composition $La_{0.7}Sr_{0.3}MnO_3$ deposited under identical conditions. For LSM thin films prepared from a diluted solution 2θ-values of 22.973, 46.932, and 73.365° are observed (Curve C, Fig. 2). From these reflections a lattice constant of 3.868 Å is calculated. As for the LCM thin film, a number of additional small reflections at 2θ-values of 32.653°, 40.391°, 58.357°, and 68.614° can be identified by XRD (Curve D) for the $La_{0.7}Sr_{0.3}MnO_3$ thin films prepared from the 0.3 M precursor solution. These can be attributed to the (110), (111), (211) and (220) reflections of the ceramic thin fim. The (100), (200) and (300) reflections can be found at angles of 22.965, 46.984 and 73.447°, with a lattice constant calculated from these values of 3.866 Å. Again, very good agreement with previously reported lattice parameters of 3.89 Å is observed [19]. Examination of these $La_{0.7}Ca_{0.3}MnO_3$ and $La_{0.7}Sr_{0.3}MnO_3$ samples from the 0.3 M precursor solution by glancing incidence XRD with an incidence angle of 1° improved the visibility of the additional small reflections with positions identical to those observed in the θ–2θ scan. These XRD patterns are shown in Fig. 3. The reflections correspond to a typical diffraction pattern of polycrystalline LCM and LSM ceramics. Due to the glancing incidence conditions, no reflections of the single crystal substrate or the thin film with orientation parallel to the substrate layers can be observed. That means that a small amount of polycrystalline material is formed when the films are deposited with solutions of higher concentrations. In order to eliminate this polycrystalline fraction, thin films have to be annealed at high temperatures for several hours.

In order to confirm the high quality of the LCM and LSM thin films from the diluted precursor solution and to exclude the possibility that only highly (100) textured, but polycrystalline thin films were prepared by our CSD technique, scanning electron micrographs of freshly broken edges of these thin films were recorded. Figure 4 shows SEM pictures of a $La_{0.7}Ca_{0.3}MnO_{0.3}$ thin film prepared by using a diluted precursor solution (Fig. 4(a)) and a 0.3 M precursor solution (Fig. 4(b)). The first film displays a very smooth surface without any grainy structure. No clear difference between substrate and thin film can be detected. On the film surface, small pores can be seen. These pores are formed during the growth process due to shrinking of the film during the heating process. In contrast to these results, the thin film from the higher concentrated precursor solution displays a clearly different structure. On the film surface, a number of small grains can be detected. In addition, the film surface has a wavy structure with some large pores. At certain points, the film loses contact with the substrate.

These results can be used to explain some aspects of the crystallization mechanism. After introducing

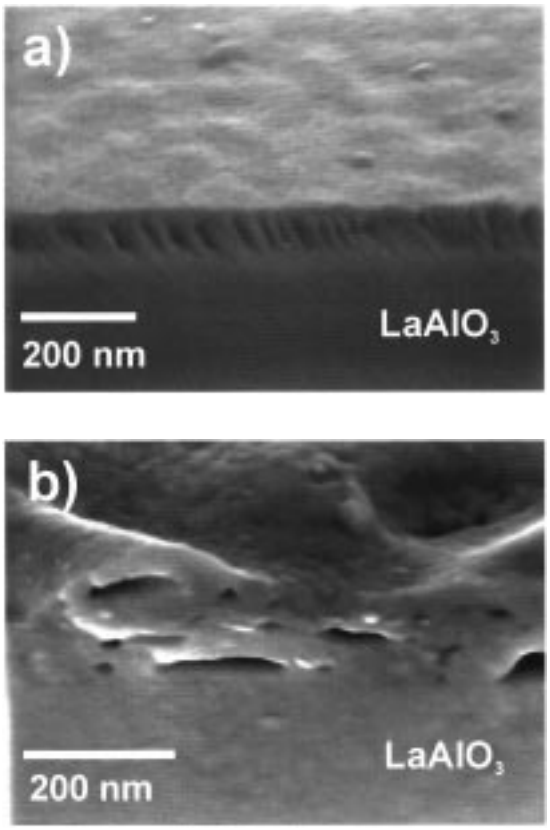

Fig. 4. Scanning electron micrographs of $La_{0.7}Ca_{0.3}MnO_3$ thin films deposited on $LaAlO_3$ substrates. (a) Thin film deposited by use of a diluted precursor solution with $c = 0.1\text{mol}^* l^{-1}$. (b) Film prepared from a precursor solution with a concentration of $0.3\text{mol}^* l^{-1}$.

the wet film into the preheated furnace, the next steps are drying of the film and the pyrolysis of organic material, leading to an amorphous film composed of carbonates or oxides. Due to the close structural relationship between substrate material $(LaAlO_3)$ and thin film, the crystallization will start at the interface layer. If the thin film thickness does not exceed a certain critical value, the crystallization front will consume the amorphous material from the bottom to the film surface before new seeds are formed at random points within the film or at the film surface. Thus, epitaxial films can be grown on single crystals if the film thickness is sufficiently small. The use of higher concentrated solutions leads to amorphous films with increased thicknesses after pyrolysis. At certain points, the crystallization process initiated at the film-substrate interface will then not be sufficiently fast to transform all the material into an epitaxial ceramic film. A small amount of misoriented, polycrystalline material can be formed caused by random crystallization in the film. This can be especially the case at points were the film loses contact with the substrate material. To eliminate this polycrystalline fraction, the thin films have to be heated to high temperatures for elongated periods of time. The driving force for this grain growth at high temperature is the elimination of grain boundaries.

These results show that the concentration of the precursor solution has a pronounced effect on the crystallographic properties of the resulting thin film and that the epitaxial growth can be achieved at lower temperatures if the film thickness is reduced

Electrical and magnetic measurements in the low-temperature regime

In order to gain an overview of the manyfold inherent properties of the manganite thin films we measured the dc resistivity versus temperature under different magnetic fields and the temperature dependence of the magnetization. As shown for the epitaxial $La_{0.7}Ca_{0.3}MnO_3$ film in Fig. 5, the resistivity reveals a typical positive temperature coeffient dependence up to its maximum at $T_{MI} = 275\,\text{K}$. The low temperature resistivity at 35 K is about 5×10^{-4} Ohm cm, which demonstrates the high quality of our CSD prepared manganite films and is comparable to resistivities of thin films deposited by PLD, MOCVD or sputtering techniques [7,11,23]. Low temperature resistivities of 1×10^{-2} Ohm cm [7]

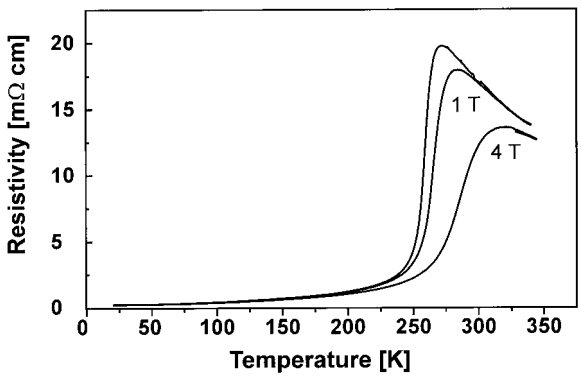

Fig. 5. Plot of the resistivity versus temperature of a $La_{0.7}Ca_{0.3}MnO_3$ thin film deposited by the use of a diluted precursor solution. Resistivity was measured without field and at $B = 1$ T and 4 T. T_{MI} is measured at 275 K.

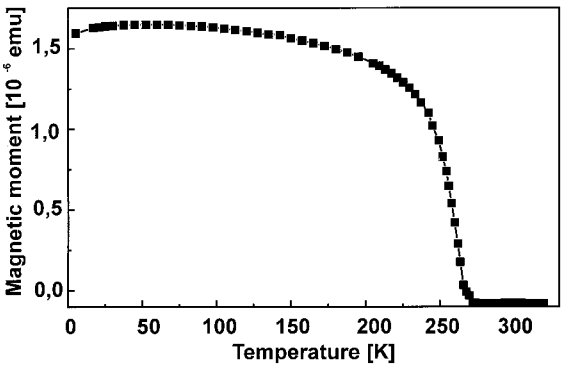

Fig. 6. Magnetic moment versus temperature of the $La_{0.7}Ca_{0.3}MnO_3$ thin film. The magnetic Curie temperature T_C of 270 K corresponds to the measured T_{MI}.

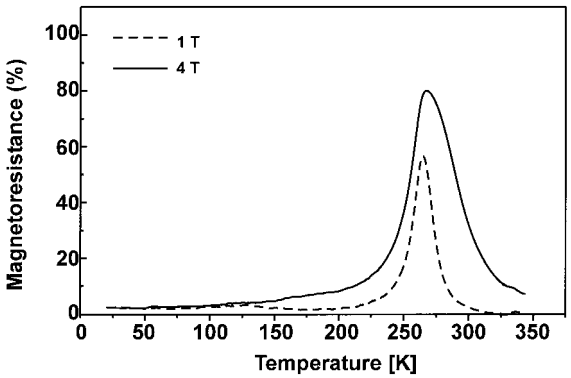

Fig. 7. Magnetoresistance ratio, determined as $(\rho(\mathrm{H}) - \rho(0)/\rho(\mathrm{H}))$, versus temperature measured at $B = 1$ T and 4 T. At 4 T, the MR ratio is about 80% at 270 K.

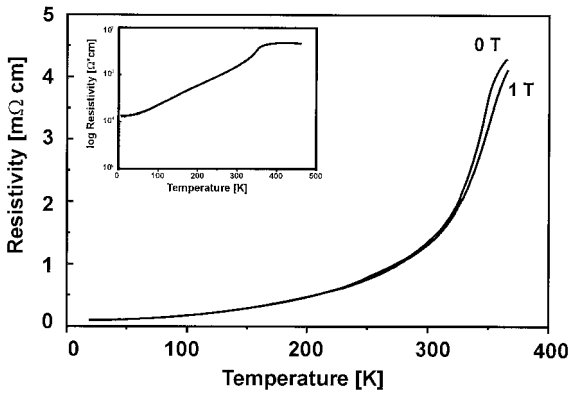

Fig. 8. Resistivity versus temperature for the $La_{0.7}Sr_{0.3}MnO_3$ thin film deposited from a 0.1 M precursor solution. Magnetoresistance was measured at $B = 1$ T. The MR effect is less pronounced for the LSM thin film than for the LCM sample.

down to 1×10^{-4} Ohm cm [11] are reported for epitaxial $La_{0.7}Ca_{0.3}MnO_3$ thin films. The resistivity at 295 K is $1.5 \times (10^{-2})$ Ohm cm, a value similar to a resistivity of $5 \times (10^{-3})$ Ohm cm reported by Hiskes [11]. The metal-insulator-transition temperature at 275 K is very close to the magnetic Curie-temperature T_C (Fig. 6) and demonstrates the coupling of ferromagnetism and electrical conductivity in these materials as was predicted by Zener [24]. The values of T_{MI} and T_C are much higher than those reported by other workers for epitaxial sol-gel derived Ca-doped manganite thin films (230 K) [12] and correspond to data for single-crystal material [11].

The magnetic field dependence of the resistivity at fields of 1 T and 4 T, respectively, is shown in Fig. 5. No magnetoresistance is measured at low temperatures, indicating that no grain boundaries are present in the thin film sample. Grain boundaries lead to a low temperature magnetoresistance as was shown in ref. [25] by the use of artificial grain boundaries. Figure 7 illustrates the magnetoresistance versus temperature as $[(\rho(0) - \rho(H))/\rho(0)]$. The maximum of the CMR effect for our LCM thin film is measured at 265 K, which is slightly below T_{MI} and T_C. To our knowledge, the *MR* ratio of about 80% for a magnetic field of 4 T is the highest value reported by now for this magnetic field.

Figure 8 illustrates the resistivity measurements for our $La_{0.7}Sr_{0.3}MnO_3$ thin film. The magnetoresistance was measured for this sample in a field of 1 T and has its maximum around 360 K corresponding to the magnetic Curie temperature T_C. This film also exhibits a small low temperature resistivity $(3 \times 10^{-4}$ Ohm cm) and a metal-insulator transition temperature T_{MI} in good agreement with reported values of single crystal thin films and bulk material [11]. The transition temperature T_{MI} at 430 K is remarkably higher than T_C in contrast to the above results for the $La_{0.7}Ca_{0.3}MnO_3$ thin films. Until now this effect is not well understood and in contrast to the theory of Zener. Nevertheless, the differences in T_{MI} and T_C seem to be an inherent property of the $La_{0.7}Sr_{0.3}MnO_3$ material and have been also described by other workers [11].

Conclusions

Highly conducting and magnetoresistive epitaxial thin films of $La_{0.7}Ca_{0.3}MnO_3$ and $La_{0.7}Sr_{0.3}MnO_3$ were

deposited by chemical solution deposition on $LaAlO_3$ (100) substrates. The growth of the thin films was influenced by the solution concentration, deposition of films by the use of diluted solutions and repeated coating-firing cycles clearly improved the quality of the crystalline film. The formation of misoriented, polycrystalline material could be avoided by influencing the thickness of the resulting thin film. A magnetoresistance of about 80% was observed in a field of 4 T around the Curie temperature T_C for the $La_{0.7}Ca_{0.3}MnO_3$ thin film.

Acknowledgment

The authors (UH, CM, RW) would like to thank the Deutsche Forschungsgemeinschaft (DFG) for financial support.

References

1. F.F. Lange, *Science*., **273**, 903–909 (1996).
2. P.A. Langjahr, T. Wagner, M. Rühle, and F.F. Lange, *Mat. Res. Soc. Symp. Proc*., **401**, 109–114 (1996).
3. A. Seifert, F.F. Lange, and J.S. Speck, *J. Am. Ceram. Soc*., **76**(2), 443–448 (1993).
4. C.W. Kwon, M.C. Robson, K.-C. Kim, J.Y. Gu, S.E. Lofland, S.M. Bhagat, Z. Trajanovic, M. Rajeswari, T. Venkatesan, A.R. Kratz, R.D. Gomez, and R. Ramesh, *J. Magnetism. Magn. Mat*., **172**, 229–236 (1997).
5. K.M. Krishnan, A.R. Modak, C.A. Lucas, R. Michel, and H.B. Cherry, *J. Appl. Phys*., **79**(8), 5169–5171 (1996).
6. P.-J. Kung, D.B. Fenner, D.M. Potrepka, and J.I. Budnick, *Appl. Phys. Lett*., **69**(3), 427–429 (1996).
7. M.F. Hawley, C.D. Adams, P.N. Arendt, E.L. Brosha, F.H. Garzon, R.J. Houlton, M.F. Hundley, R.H. Heffner, Q.X. Jia, J. Neumeier, and X.D. Wu, *J. Cryst. Growth*., **174**, 455–463 (1997).
8. S. Freisem, A. Brockhoff, D.G. de Groot, B. Dam, and J. Aarts, *J. Magnetism. Magn. Mat*., **165**, 380–382 (1997).
9. B.W. Chung, E.L. Brosha, F.H. Garzon, I.D. Raistrick, R.J. Houlton, and M.E. Hawley, *J. Mat. Res*., **10**(10), 2518–2522 (1995).
10. J. J. Heremans, M. Carris, S. Watts, X. Yu, K. H. Dahmen, and S. von Molnár, *J. Appl. Phys*., **81**(8), 4967–4969 (1997).
11. G. J. Snyder, R. Hiskes, S. DiCarolis, M.R. Beasley, and T. H. Geballe, *Phys. Rev. B*., **53**, 14434–14444 (1996).
12. S.-Y. Bae and S.X. Wang, *Appl. Phys. Lett*., **69**(1), 121–123 (1996).
13. T. Manabe, I. Yamaguchi, W. Kondo, S. Mizuta, and T. Kumagai, *J. Mat. Res*., **12**(12), 541–545 (1997).
14. R. von Helmolt, J. Wecker, B. Holzapfel, L. Schultz, and K. Samwer, *Phys. Rev. Lett*., **71**(14), 2331–2333 (1993).
15. S. Jin, T.H. Tiefel, M. McCormak, R.A. Fastnacht, R. Ramesh, and L.H. Chen, *Science*, **264**, 413–415 (1994).
16. J.A. Brug, T.C. Anthony, and J.H. Nickel, *MRS Bulletin*, **5**, 23–27 (1996).
17. H. Lemme, *Elektronik*, **3**, 40–50 (1998).
18. R. Mahesh, R. Mahendiran, A.K. Raychaudhuri, and C.N.R. Rao, *Appl. Phys. Lett*., **68**(16), 2291–2293 (1996).
19. J.Y. Gu, C. Kwon, M.C. Robson, Z. Trajanovic, K. Ghosh, R.P. Sharma, R.P. Sharma, R. Shreekala, M. Rajeswari, T. Venkatesan, R. Ramesh, and T.W. Noh, *Appl. Phys. Lett*., **70**(13), 1763–1765 (1997).
20. N.-C. Yeh, C.-C. Fu, J.Y.T. Wei, R.P. Vasquez, J. Huynh, S.M. Maurer, G. Beach, and D.A. Beam, *J. Appl. Phys*., **81**(8), 5499–5501 (1997).
21. J.Q. Guoi, H. Takeda, N.S. Kazama, K. Fukamichi, and M. Tachiki, *J. Appl. Phys*., **81**(11), 7445–7449 (1997).
22. U. Hasenkox, C. Mitze, and R. Waser, *J. Am. Ceram. Soc*., **80**(10), 2709–2713 (1997).
23. A. Gupta, G.Q. Gong, G. Xiao, P.R. Duncombe, P. Lecoeur, P. Trouilloud, Y.Y. Wang, V.P. Dravid, and J.Z. Sun, *Phys. Rev. B*., **54**(22), R15629–15632 (1996).
24. C. Zener, *Phys. Rev*., **82**(3), 403–403 (1951).
25. N.D. Mathur, G. Burnell, S.P. Isaac, T.J. Jackson, B.-S. Teo, J. L. MacManus-Driscoll, L.F. Cohen, J.E. Evetts, and M.G. Blamire, *Nature*., **387**, 266–268 (1997).